CHAPTER 18

Emergency Core Cooling—Blowdown

F. Mayinger

1 INTRODUCTION

For light water reactors, the break of a large pipe filled with primary coolant is regarded as the maximum credible accident (MCA). For this case, it has to be guaranteed that all the components subject to pressure can withstand the strain, and that the core is cooled short- and long-term. The stored heat of the fuel rods as well as the heat that is developed in the core after a shutdown have to be carried away. Without coolant, or with decreasing heat-transfer coefficients, the temperature of the rods may increase rapidly to undue values. The mechanical strain of the primary components as well as the temperature of the core are calculated by computer programs, which utilize experimental results.

For the necessary thermohydraulic studies, one of the most important questions is that of the critical mass flow rate, defining the time until the primary system is empty; that means the remaining time for the cooling of the fuel rods. Besides this, it is necessary to know exactly the forces caused by the blowdown and acting on the primary components. There may be vibrations induced that are caused by the pulsating flow in the jet, which can cause damage to the system. Finally, the mutual influences of the flow inside the four loops—broken or unbroken—are of interest. The behavior of the feed pumps and the steam generators are of special importance.

In spite of the considerable research work, the thermal behavior of the core is still the central question of the LOCA. For detailed knowledge of the time delay between the rupture of the pipe and the beginning of DNB as well as of the heat transfer in the postburnout region, experimental work has to be executed before a theoretical treatment or numerical calculations in computer programs are possible. Both incidents—onset of DNB and postburnout heat transfer—fix the level of temperature that will occur for stagnating or totally evaporated coolant at the end of the blowdown region. To enlarge the knowledge of these dangerous situations, a great number of blowdown

experiments have been undertaken by the research program of the FRG. The experiments were executed for different geometries. They were carried out under spontaneous and--for an exact parametric comparison of burnout and heat-transfer behavior--controlled conditions. Experiments at KWU Grosswelzheim were done with water as coolant in four-rod clusters and 25-rod clusters (AEG-Bericht, 1971). For larger rod clusters, like those used in nuclear reactors, one needs a lot of energy (for example, 10 MW for the 50-rod cluster). That is why, parallel to this program, experimental work with R12 as the modeling fluid was started (Belda and Viert, 1974a). The aim is to test great rod clusters for steady state and transient burnout and heat-transfer conditions. The tests are planned with clusters of up to 64 rods.

2 WATER EXPERIMENTS

2.1 Test Loops

For the performance of the blowdown experiments with water, two test loops were used at KWU Grosswelzheim. Figure 1 shows the loop for inside cooled tubes and four-rod clusters. The experiment was executed in such a way that, after fixing the reactor steady-state conditions in the test-loop, the burst disc

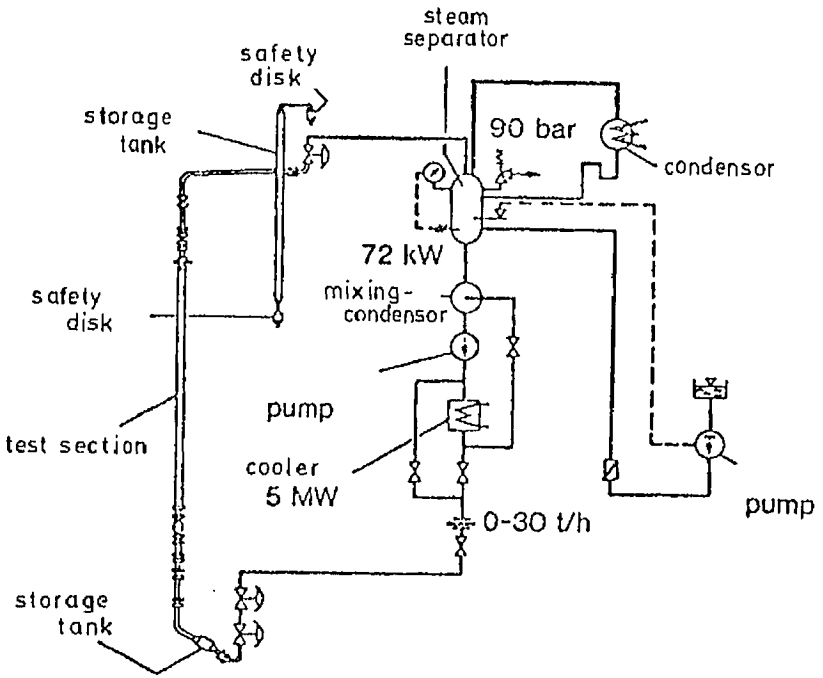

FIG. 1 Test loop circuit for blowdown test of inside cooled tubes and four-rod clusters.

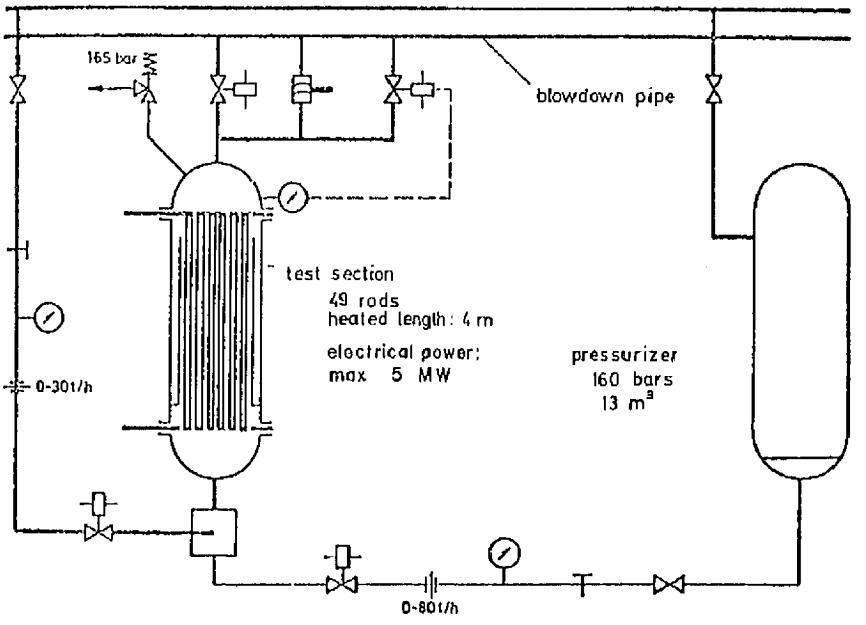

FIG. 2 Circuit diagram for rod-cluster measurement test loop.

was destroyed. Simultaneously, the test section was separated from the loop by quick-closing valves. Clearly defined starting conditions were reached, but not exactly the same situation as in a nuclear reactor because of the stagnating mass flow just before blowdown.

For the measurement of the transient mass flow rate during the blowdown, a combination of orifice, turbine-flowmeter and γ-ray testing was used. The double information on the mass flow rate measured with the flowmeter and the orifice was combined with the γ-ray attenuation to control the result. The deviation between the two results was less than 10 percent (AEG-E3-2560, 1972).

In Fig. 2, the test loop for the rod-cluster measurements (25 and 49 rods) is shown. This kind of open test loop was chosen to be able to control the mass flow rate at the entrance. Thus, inlet conditions of the fluid are guaranteed by mixing subcooled water with steam. In this test loop, the heat-transfer behavior of the test section is not influenced by the characteristics of the loop. So, for a theoretical treatment of the results, one obtains simple conditions that are easy to control.

2.2 Program for Water Experiments

To further the aim of the research program, i.e., to find out the burnout delay time and the heat-transfer conditions, the location and cross-section of the break area and the heat-flux behavior were varied greatly.

In the experiments with the internally cooled tubes, which were similar to PWR conditions (pressure in the beginning, 90 bar; stationary subcooling at the entrance, 20K; stationary heat-flux density, 165 W/cm^2; void fraction up to 5 percent), the cross section of break was varied from 0.2F to 2F.

Besides this, the proportion between the cross-section of break in the hot and the cold legs was varied (1:0, 3:1, 1:3, 0:1). The heat-flux density was fixed first at 40 percent of the nominal value at the moment of break, and second, it was lowered 1.2 s after the break.

From these experiments, one can expect detailed knowledge of the influence of different parameters.

The experiments with the four-rod clusters were carried out with boiling-water reactor conditions. Because of the given design of this reactor, only small breaks have to be expected. Furthermore, there has to be investigated not only a break-location at the test-section exit but, in addition, a water storage just before the break must be simulated and, therefore, varied in the tests.

An exact scaling of reactor behavior with this test section was not possible because the pump, necessary for simulation of flow conditions, was shut down during the tests; but an inlet mass flow was realized to some degree by closing the valve before the lower plenum within 0.7 s. Then, differences in results, mainly in DNB delay, compared to tests with an immediately closed valve must be related to simulated inlet mass flow. In these experiments, the pressure in the beginning was 70 bar, the steady-state heat flux was maximally 110 W/cm^2, and the initial void fraction was 40 percent.

2.3 Results

In Fig. 3, for the inside cooled tube, the pressure is plotted versus time with the break area as a parameter. Of course, for smaller break areas, the pressure gradient is smaller, too. One can see that, for the same total cross-section of break, there are different pressure gradients for different locations of break. If the cross-section at the test-section exit is larger (curves I and II), the pressure level decreases rapidly to saturation pressure. The reason is the initial void fraction of 5 percent, which permits a high flow of volume through the break.

With large break areas in the subcooled region (at test-section entrance), there is a more steady pressure gradient, since the initially subcooled flow then is a homogeneous two-phase mixture.

With this high water-flow rate, after a certain time the pressure gradient becomes greater than for the location of break in the hot leg. The behavior of the mass flow rate and the void fraction plotted against time (see Fig. 4) is characterized by the closing of the valve and the opening of the burst disc.

For breaks in the hot leg, for example, the mass flow through the lower plenum is interrupted quickly. A remarkable flow through the core is occurring only when the pressure decreases to a level where the liquid in the

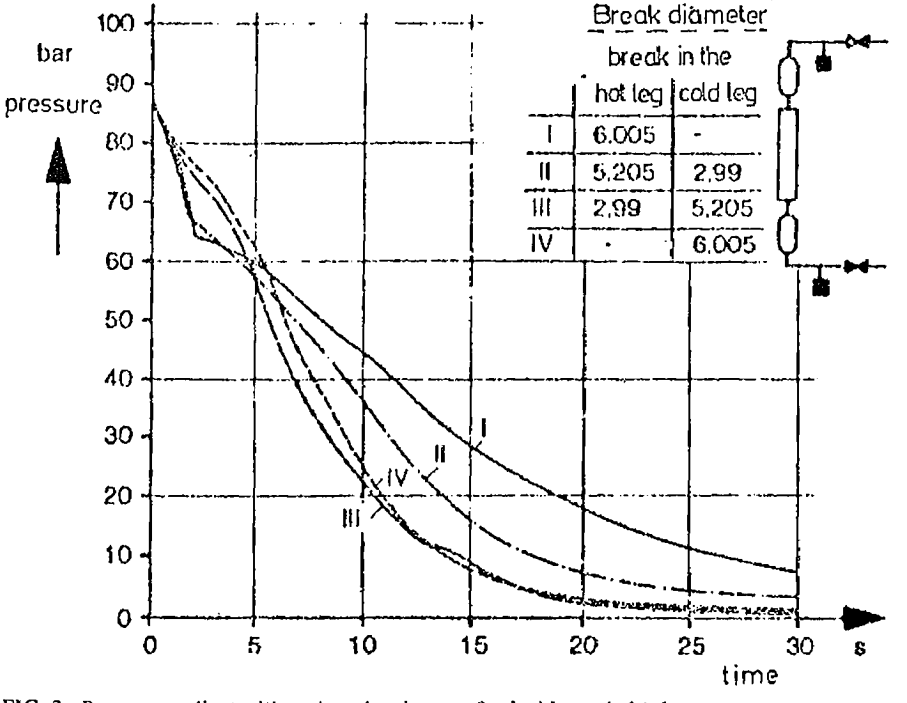

FIG. 3 Pressure gradient with various break areas for inside cooled tube.

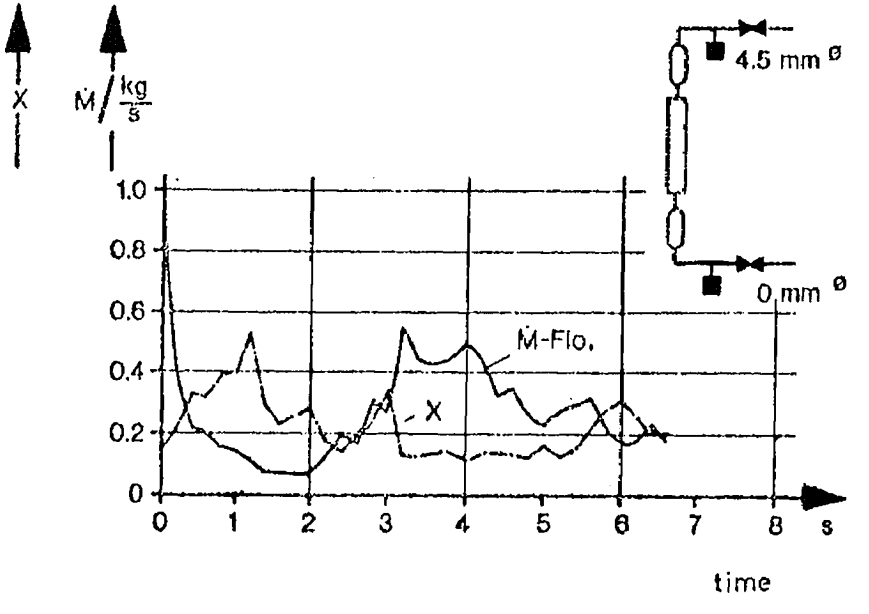

FIG. 4 Mass flow rate and void fraction vs. time (approximation).

lower plenum is flashing. The void fraction behaves anticyclic to the mass flow rate. That indicates that the mass flow rate is strongly dependent upon the liquid content in the circuit.

Of course, the strong gradient of the mass flow rate during the first second is not similar to the conditions in the reactor. The gradient is caused by shutdown of the valve, which is specific for the loop.

2.3.1 *DNB Results*

The gradients for the pressure, the mass flow, and the void fraction are essential for the interpretation of the heat-transfer behavior and the onset of DNB. Both can be taken from the curve of wall temperature and the corresponding fluid temperature. That is why the inside cooled tube was equipped with 14 thermocouples distributed equally over the heated length. With this, not only the time dependence but also the local behavior of the DNB can be proved, and this is of special interest for nonuniformly heated rod clusters.

Figure 5 shows the wall temperatures of DNB rods versus time for different break conditions. The break area is varied between the cross section of two main pipes (2F) of the primary circuit and 0.2F. The position where the plotted temperature was measured is indicated by an arrow in the figure.

Qualitatively, one can see from this figure that the area of a break in the hot leg has almost no influence on DNB delay time whereas, in the cold leg, there is a strong effect with large break areas. The position of the break

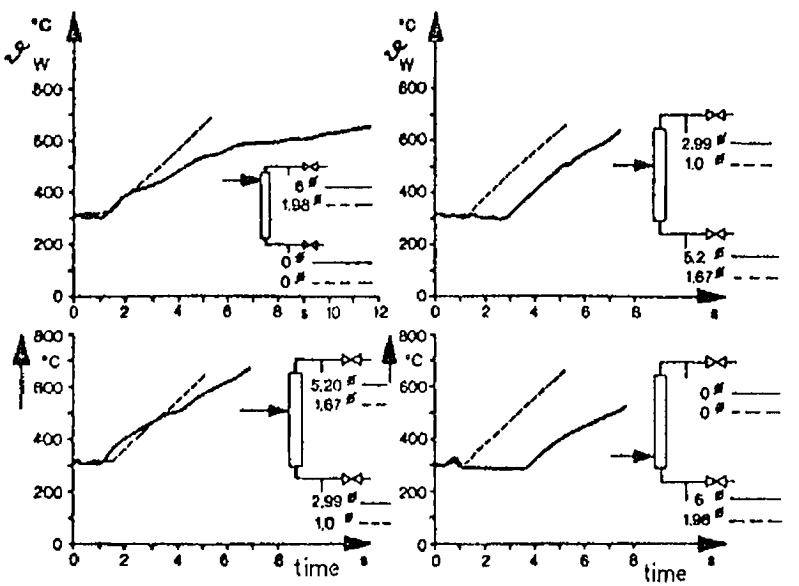

FIG. 5 Wall temperature of DNB rods vs. time for different break conditions.

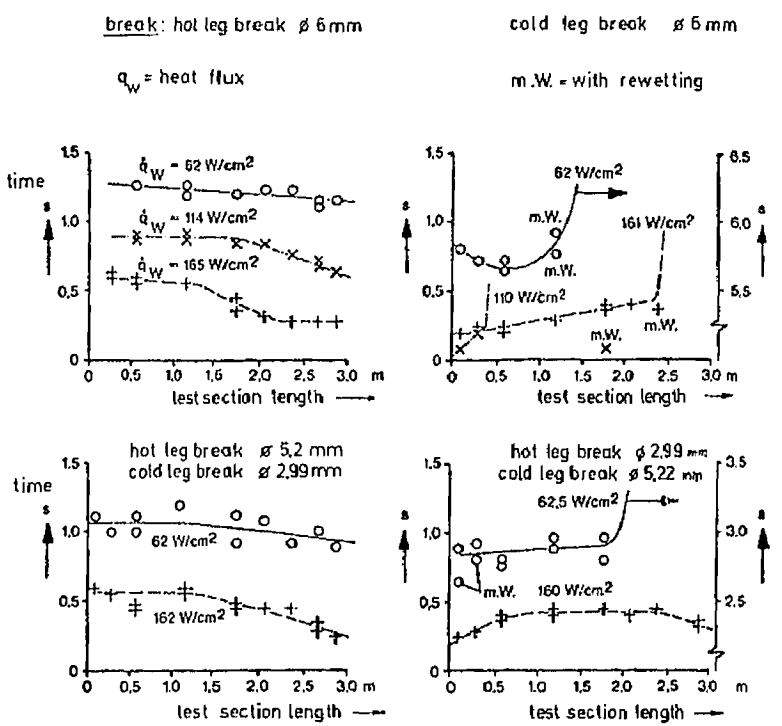

FIG. 6 Influence of heat-flux density and heated length of rod on DNB delay.

influences the burnout behavior only if there are large broken areas. The reason for this behavior can be found in the time-dependent pressure and mass flow rate in the core during the blowdown. With small break openings, there is only a negligible acceleration resulting from the pressure drop caused by the break. This means that the vapor generated in the core is not carried away fast enough, so the local quality in the fluid is rapidly increased, which promotes the onset of an early DNB.

With large break areas, the flow is strongly accelerated. One has to be aware, however, of the fact that, with a break in the cold leg, the flow is reversed and the steam just produced influences the DNB behavior in the direction of an earlier burnout. A break in the hot leg does not generate a flow return and subcooled fluid still enters the core, but now with much higher velocity. So the DNB is considerably delayed. This effect is supported by the flashing of the water in the core at the beginning of the blowdown, which results in a better cooling of the fuel rods.

From Fig. 5, one can see that the DNB delay time falls between 1 and 4 s, depending on the thermohydraulic conditions. The experimental parameters presented in this figure correspond to the conditions in a pressurized water reactor.

Figure 6 shows how the temperature gradient of the wall depends on the

heated length of the rod. To be exact, one has to say that, in these tests, the inner wall temperature of an electrically heated rod was measured, but the error in DNB response time caused by this was only 0.05 s, so that the sharp change in the temperature curve is almost identical with the onset of burnout. Compared to Fig. 5, discussed earlier, Fig. 6 now gives, in addition, the influence of the heat-flux density on the DNB delay. With increasing heat flux, the time between the beginning of blowdown and DNB becomes shorter, which easily can be explained by the fact that the liquid wetting the wall is now evaporating faster. In addition, with increasing heat-flux density, there is a stronger dependency of the DNB delay from the break position. There are two reasons for this: first, the steam quality in the core at the beginning of the blowdown is now higher and, second, the evaporating effect is stronger.

An interesting insight into the problem of DNB behavior is given in the histogram shown in Fig. 7. Here the frequency, in the sense of a probability of DNB occurrence, is plotted against the integrated heat addition, i.e., versus total added energy (qt) until onset of burnout. From this figure, one can see that there is a probable total energy addition which has to be transferred to the fluid until burnout occurs. A simple correlation shows that only a small part of the heat is stored in the wall; most of it is used to heat up and evaporate the liquid. Using a simple DNB model, one can calculate roughly that there has to be evaporated a liquid layer of about 0.1-0.2 mm thickness until the wall temperature rises because of DNB. With high subcooling, the DNB time is a little longer because of heating up the liquid to the saturation point.

From these results, one can see that it is not correct to calculate the DNB delay from quasi-steady-state burnout correlations. In the experiments shown

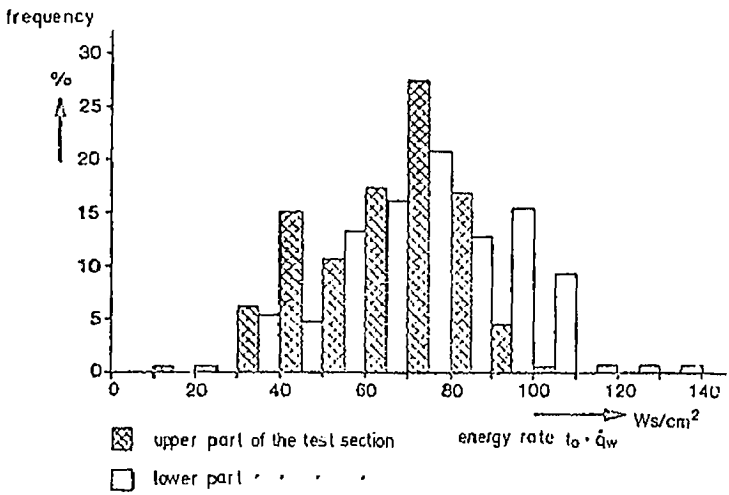

FIG. 7 Probability of DNB occurrence as related to total added energy.

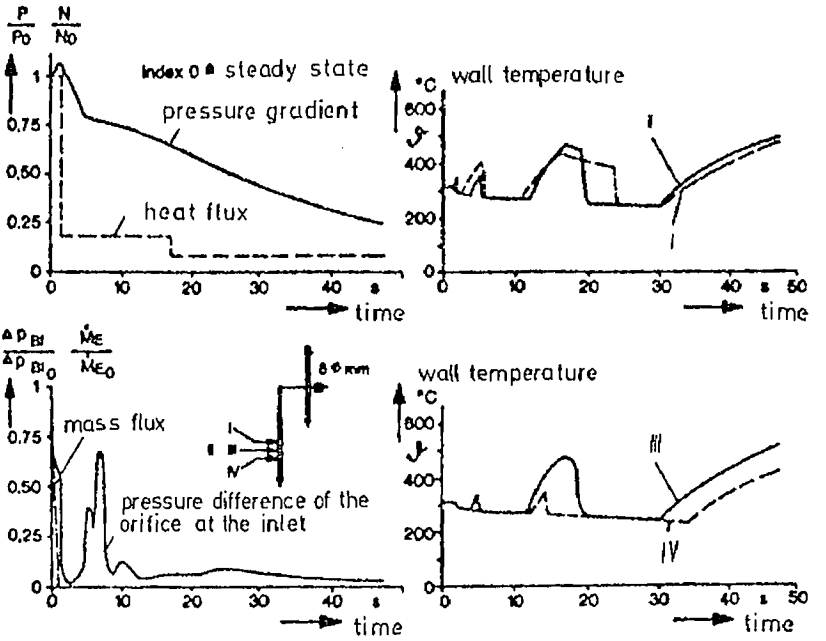

FIG. 8 Rewetting and wall temperature vs. time for four-rod bundle.

in Fig. 7, the mass flow rate just before the beginning of the blowdown was blocked by closing a valve, so the DNB should have started immediately, according to quasi-steady burnout considerations.

2.3.2 Rewetting

The question arises as to whether there is a rewetting shortly after the first DNB-onset, i.e., whether there is more likely a burnout- or a dryout-behavior. The measurements showed that rewetting really occurs if BWR conditions prevailed before the blowdown. Such tests were made primarily with four-rod clusters at the KWU in Grosswelzheim (KWU/R5-2885, 1974). The rewetting after the first DNB is clearly indicated in Fig. 8 where, in the diagrams on the right-hand side, the behavior of the wall temperature versus time is plotted.

Usually it is assumed that rewetting cannot start as long as the wall temperature is above the Leidenfrost point. In a large number of experiments—not only for nuclear reactors—the Leidenfrost-temperature was measured, pointing out that it is usually about 50–110 K higher than the saturation temperature of the liquid at the given pressure. If one plots the rewetting conditions during the blowdown experiments in a histogram, as shown in Fig. 9, one can see that there is very frequently a rewetting at temperatures of 150-250 K, which is not in accordance with steady-state measurements. Up to now it has not been clarified why rewetting during

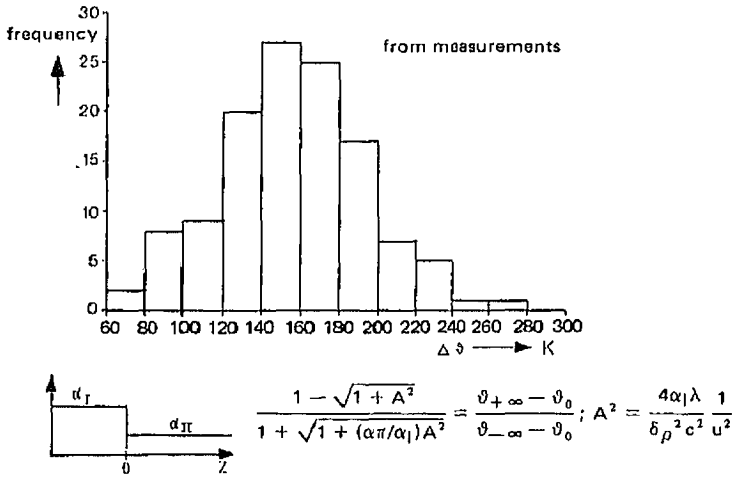

FIG. 9 Temperature vs. rewetting conditions during blowdown.

blowdown can occur at these high temperatures, but the effects are of high interest for the safe layout of the core, because of the high energy reduction in the rod.

One reason for the rewetting could be the strong acceleration and the higher subcooling of the liquid entering the core from below. In addition, there may be, depending on the area and the location of the break, a flashing of the fluid in the core, which improves the heat transfer behavior.

2.3.3 Postdryout Heat Transfer

From the time-dependent temperature behavior of the heated wall, one can calculate the heat-transfer coefficient using the well-known Fourier equation. For experimental reasons, the time after blowdown, until which the heat-transfer coefficient can be measured, is limited by the maximum allowable wall temperature at which the heat input to the wall has to be switched off.

In Fig. 10, heat-transfer coefficients are plotted which were taken in tests of inside cooled tubes. In this figure, different conditions for break areas and break locations are given. There is a remarkable reduction of the heat-transfer coefficient immediately after DNB.

The heat-transfer coefficient in the postdryout region during blowdown is strongly dependent on break area, which governs the flow conditions in the core. As expected with large break areas, the heat transfer is quite good because of the high acceleration of the vapor-liquid mixture in the core. In this period, heat-transfer coefficients reach values between 1000 and 2500 W/m^2-K, whereas with small break areas, the heat-transfer coefficient goes down to 500 W/m^2-K.

Figure 11 shows results of a test with a 4-rod bundle, where the break area

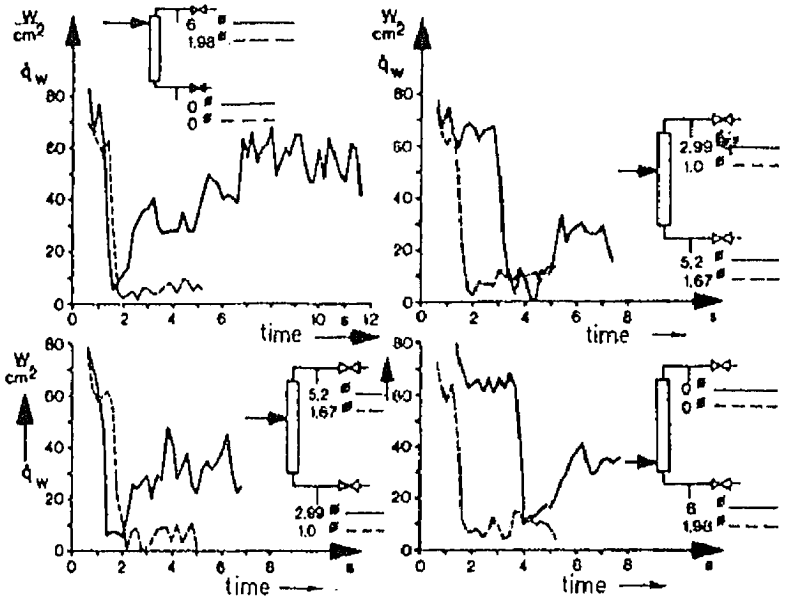

FIG. 10 Heat-transfer coefficient vs. time for various break conditions.

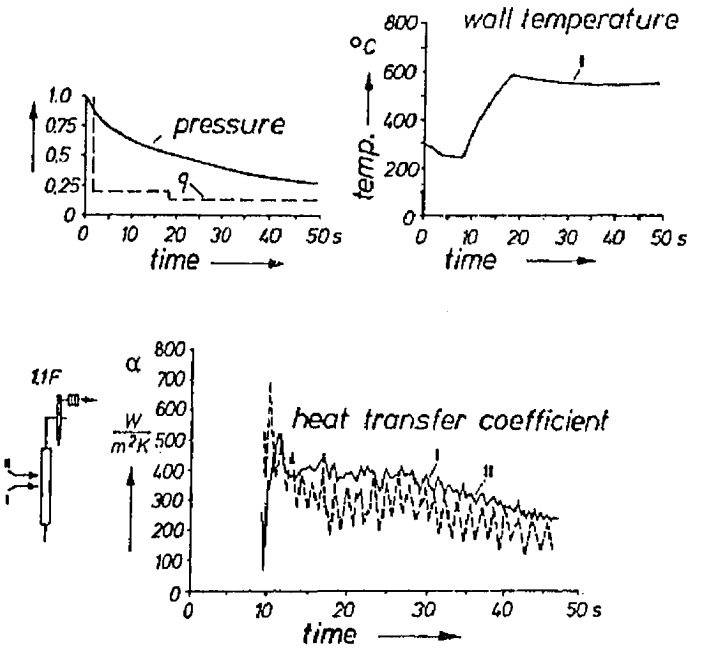

FIG. 11 Test results with four-rod bundle; break area corresponds to cross section of one main pipe of primary circuit.

corresponds to the cross-section of one main pipe of the primary circuit (1F). Imitating the decay-heat after scram, the heat flux of the rods was lowered during the test after 1.5 s from 100 to 18.5 percent, and after 17 s to 10 percent. The DNB delay time was 9 s in this test, as one can see from the behavior of the wall temperature. There is a relatively small temperature gradient in the time between 17 and 50 s. This means that the heat added is almost equal to the heat removed. The heat-transfer coefficient in the postdryout region is about 500 W/m^2-K at the beginning, and drops down later with decreasing mass flow rate in the core to 250 W/m^2-K. With smaller break areas, the heat-transfer coefficients lay between 100 and 250 W/m^2-K.

3 MODELING EXPERIMENTS WITH FREON 12

At the beginning of this chapter, it was mentioned that, in addition to the tests done at KWU/Grosswelzheim with water, there were carried out experiments with Freon 12 as cooling fluid. Because of the high heat-flux densities in water, which need a high power supply, the number of fuel rods to be tested is limited to about 25. Using freon as a modeling fluid, one has the benefit of much smaller heat-flux densities—they are lower by a factor of approximately 20—which also makes it possible to test clusters with a large number of rods. In addition, the cost of the experiments can be greatly reduced and, because of the much more convenient experimental conditions, the time needed for carrying out the measurements is much shorter.

For scaling up the freon tests to the water conditions given in the reactor, one has to work out modeling laws by theoretical calculations strongly supported by comparison experiments. It would go into too much detail to explain here these scaling laws. Therefore, it should be pointed out that, in Fig. 12, the blowdown conditions in water and in Freon are really similar, as one can see from comparing the behavior of pressure, mass flow rate, and void fraction of water and Freon.

The scaling theory for blowdown can be based on the well-known modeling laws given in the literature for steady-state burnout. But for reducing and adjusting the thermodynamic properties of the two fluids, it is advantageous not to use the same density ratio between vapor and liquid but, according to the theorem of the corresponding states, to make the reduction with the help of the critical properties. A comparison of thermodynamic properties reduced in this way (especially of the latent heat of evaporation, the specific heat, and the viscosity) gives a better correspondence in the whole pressure region occurring during blowdown (Belda and Viert, 1974a).

Using the same reduced pressure, p/p_k, the absolute pressure in the Freon tests is much smaller than in water. This means that one has to lower the outside pressure for the Freon test appreciably to get the same accelerating forces under both conditions. This can be done by condensing the Freon vapor, after leaving the break, in a large vessel filled with heat-transfer

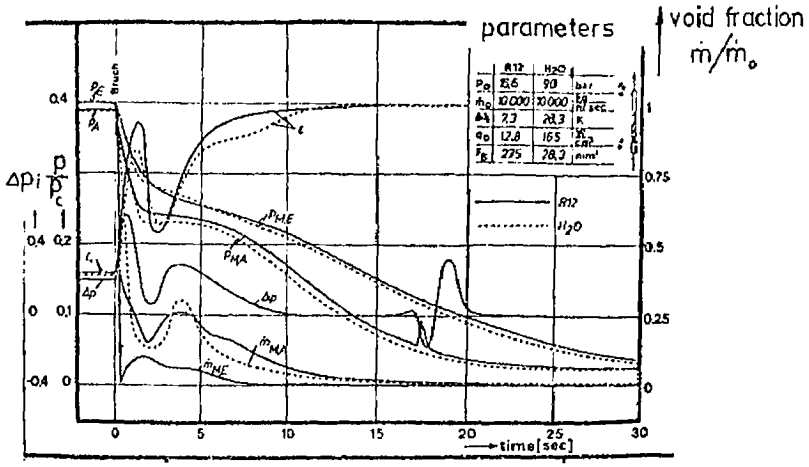

FIG. 12 Modeling tests on reactor emergency cooling: comparison of blowdown conditions in water and in R12.

components that are cooled down to −70°C. Thus, one can reproduce the flow conditions in the Freon tests completely. The scaling laws for these blowdown tests are given in Belda and Viert (1974a).

With Freon as a modeling fluid, tests were done to investigate the DNB delay behavior (Belda and Viert, 1974b). To get a clear insight into the problem, a systematic variation of all influencing parameters was applied by varying only one and keeping all others constant. The tests reproduced mainly boiling water reactor conditions. The parameters varied were

heat-flux density
break area
inlet subcooling
initial pressure
mass flow rate before blowdown

In Fig. 13, the dependency of the DNB delay time is plotted against different thermohydraulic parameters. The DNB delay time is defined as the time difference between the opening of the burst disc and the first temperature rise due to burnout. The parameters chosen are initial pressure of the system, mass flow rate, and inlet subcooling. In spite of the fact that these parameters are varied in large ranges a variation of the DNB delay time was measured only between 0.5 and 1.2 s, which shows the small influence of these variables on the DNB delay.

The measurements shown in Fig. 13 are representative for a break in the hot leg, but there would not be too much difference for a cold leg break.

There is a higher influence of the break area on the DNB delay, as

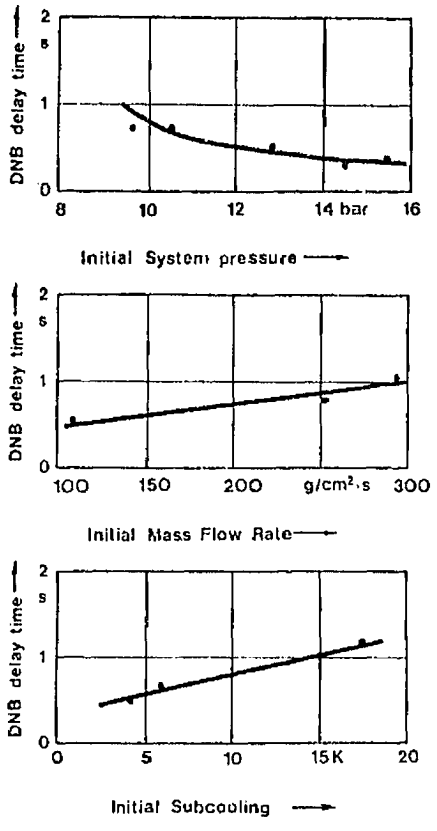

FIG. 13 Burnout delay time as a function of various thermohydraulic parameters.

demonstrated in Fig. 14. With decreasing break area, the pressure gradient in the first seconds of the blowdown becomes smaller, and so the acceleration of the cooling fluid is not so high. Because of this acceleration and the following high-velocity steam flow there definitely occurs an entrainment of the liquid film at the wall, which is lower with less acceleration at smaller break area, so the DNB occurs later.

The highest influence on the DNB delay time is, however, the heat-flux density. This is clearly shown in water tests as well as in Freon experiments. The heat-flux density does not only control the amount of evaporated liquid during the blowdown, but also the initial void near the wall before blowdown. Under boiling water reactor conditions, there is annular flow in the core, which means that only a thin liquid film exists at the wall for cooling. Only this thin film is available for evaporation after blowdown, before DNB occurs.

Figure 15 shows that also for a cold leg break, the area of the leak and the heat-flux density highly influence the DNB delay time. Compared to a hot leg break, the dependency is a little smaller. The DNB delay time dependent on these parameters varies between 1 and 3 s.

Also the postdryout heat-transfer behavior is very similar in water and in

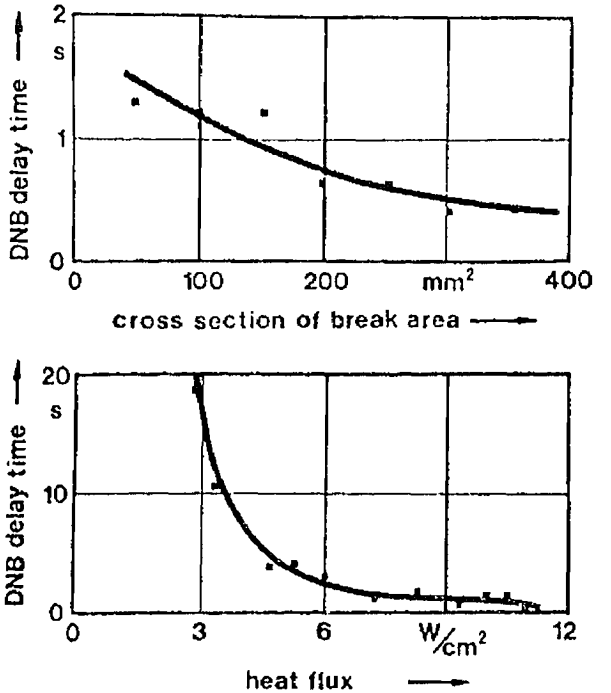

FIG. 14 Burnout delay time as a function of break area and heat-flux density for a hot leg.

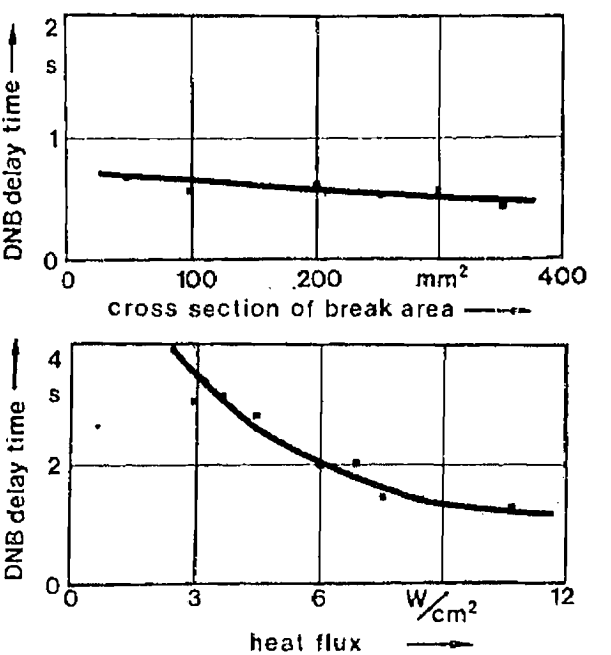

FIG. 15 Burnout delay time as a function of break area and heat-flux density for a cold leg.

Freon, and there can be drawn a unique relationship between the important parameters. The most dominating variable is the break area, because it control the flow-rate conditions and the acceleration in the core. From the experimental results for the heat-transfer coefficient plotted in Fig. 16, one can see that, with small break areas, the values are much lower than with large ones. The heat-transfer coefficients now fall between 300 W/m^2-K (1/10F and 500 W/m^2-K (2F). If we express the heat-transfer behavior in terms of Nusselt numbers we get values between 300 and 500, which corresponds to the conditions in water.

The variation of the other parameters did not give a clear dependency on the heat-transfer coefficient. In Fig. 17, for example, the heat-transfer coefficient versus time is plotted with the heat-flux density as a parameter. There is a strong dependency on the burnout delay time but almost no influence on the heat-transfer coefficient. After DNB, the measured heat transfer coefficients in this figure all were about 500 W/m^2-K. The break area corresponded to a 2F leak.

4 THEORETICAL CALCULATION MODELS

4.1 DNB Model

The test results gained can be reproduced satisfactorily by very simple calculation models for both investigation aims: onset of DNB and post-DNB heat transfer.

Starting from considerations of DNB with annular flow present at initial BWR conditions, steady-state dryout will occur if film flow rate decreases

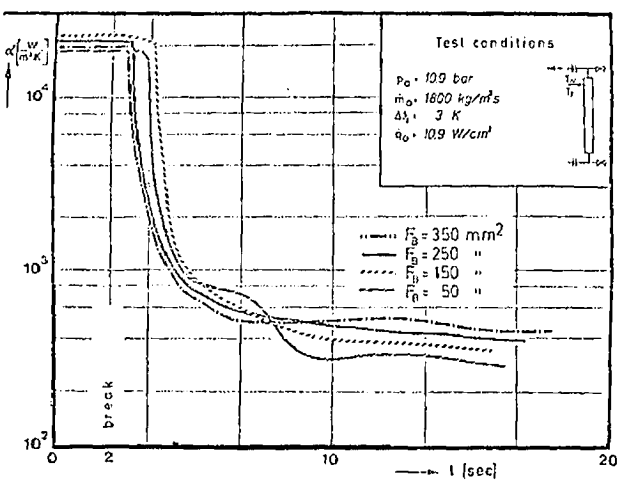

FIG. 16 Modeling tests on reactor emergency cooling: heat-transfer coefficient vs. time; dependence upon break area.

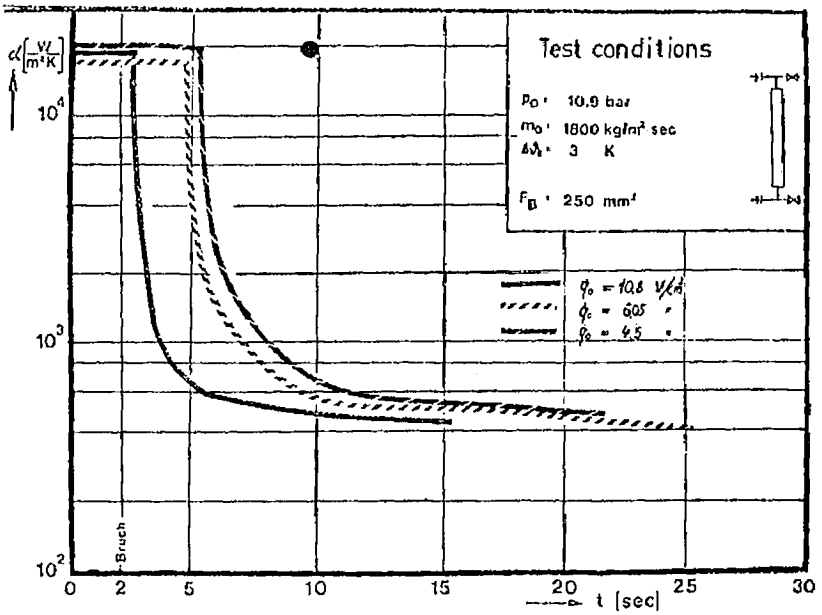

FIG. 17 Modeling tests on reactor emergency cooling: heat-transfer coefficient vs. time; dependence upon heat-flux density.

zero. Similarly to stationary conditions during pressure transients, the liquid film diminishes because of heat input with connected evaporation. But, additionally, there must be taken into consideration the strong acceleration of the vapor flow in the channel center, causing liquid entrainment.

$$\frac{\partial M_{\text{film}}}{\partial t} = \left(\frac{\partial M}{\partial t}\right)_{\text{heat add}} + \left(\frac{\partial M}{\partial t}\right)_{\text{entr}} \tag{1}$$

Decreasing of film flow rate because of heat input can be calculated by

$$\left(\frac{\partial M}{\partial t}\right)_{\text{heat add}} = -\frac{\dot{Q}_{\text{ad}}}{h} \tag{2}$$

where h = latent heat of evaporation. The momentum exchange equation gives information about the influence of the vapor flow on liquid film. According to some authors (Dukler, 1961; Paleev and Filipovich, 1965; Truong-Quang Minh, 1965), it is suitable to calculate liquid entrainment as a function of pressure gradient:

$$\frac{\partial}{\partial t}\left(\frac{\partial M}{\partial t}\right)_{\text{entr}} = CA_{\text{film}}\frac{\partial p}{\partial z} \tag{3}$$

The factor C includes all forces neglected in the momentum exchange equation, e.g., shear stress and gravitational forces. The decreasing of the liquid mass in the film can be expressed by partial differentiation:

$$\frac{\partial M_{\text{film}}}{\partial t} = \frac{\partial(\rho_l V)}{\partial t} = \pi L\left[(D\delta - \delta^2)\frac{\partial \rho_l}{\partial t} + \rho_l D\frac{\partial \delta}{\partial t} - \frac{\partial(\delta^2)}{\partial t}\right] \quad (4)$$

where δ = film thickness. The equations inserted in the first one leads to

$$-\frac{\partial(\delta^2)}{\partial t} + \frac{\partial(\delta)}{\partial t}D - \frac{\delta^2}{\rho_l}\frac{\partial \rho_l}{\partial t} - \frac{\delta D}{\rho_l}\frac{\partial \rho_l}{\partial t} = \frac{Q_{\text{ad}}}{\pi L r \rho_l} - \frac{CD}{4L\rho}\int(1-\epsilon)\frac{\partial p}{\partial z}dt \quad (5)$$

Because of the integral on the right-hand side, no complete solution of this differential equation is possible, but the computer codes used at the time for the high-pressure range of blowdown give approaches for void fraction and pressure drop as a function of time and length, so that numerical integration can be conducted for small time intervals. With the boundary conditions: that the film thickness at $t = 0$ s corresponds to the initial one and at $t = t_{\text{DNB}}$ it is zero, one gets an equation for dryout delay:

$$t_{\text{BO}} = \frac{-\rho_l}{\frac{\partial \rho}{\partial p}\frac{\partial p}{\partial t}} \ln\left\{\frac{\frac{Q_{\text{ad}}}{\pi DLh} + \frac{CD}{4L}\left[\int(1-\epsilon)\frac{\partial p}{\partial z}dt\right]t_{\text{BO}}}{\frac{Q_{\text{ad}}}{\pi DLh} + \delta_0\frac{\partial \rho_l}{\partial p}\frac{\partial p}{\partial t} + \frac{CD}{4L}\left[\int(1-\epsilon)\frac{\partial p}{\partial z}dt\right]t_{\text{BO}}}\right\} \quad (6)$$

which must be solved iteratively. For modeling tests with Freon, DNB results can be well verified with $C = 0.15$ (Fig. 18).

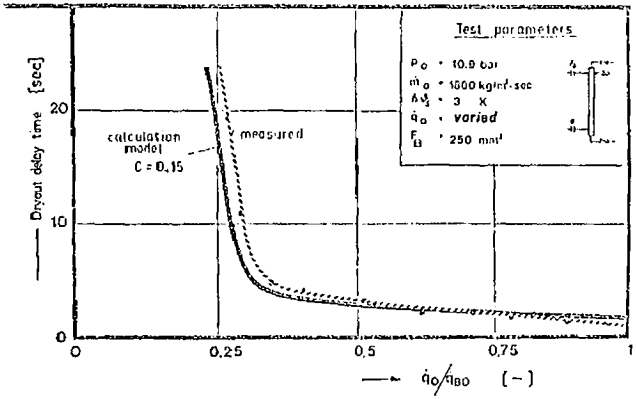

FIG. 18 Scaling tests on reactor emergency core cooling: burnout delay time using R12; $C = 0.15$.

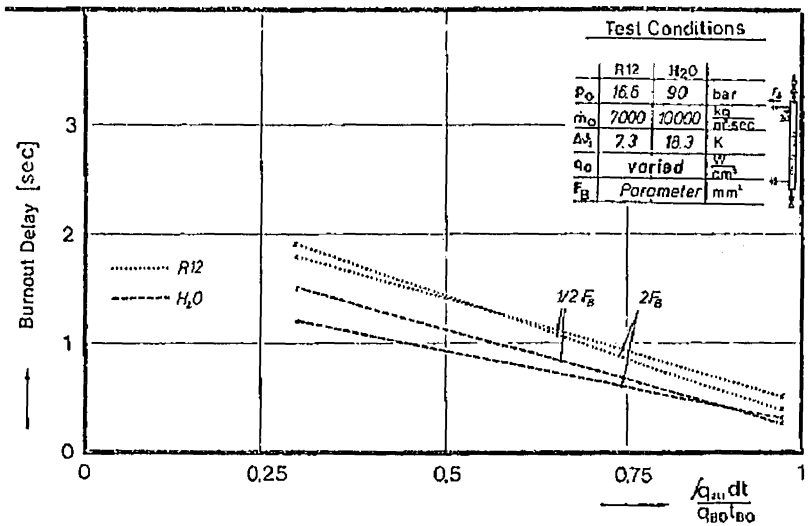

FIG. 19 Burnout delay time for hot leg break: comparison of test results in water and in R12.

In contrast to water, DNB occurs later in Freon. For a hot leg break, corresponding test results are compared in Fig. 19. For water conditions, DNB delay times can be reproduced in quite as good a manner as in Freon by choosing the constant as $C = 0.6$.

4.2 Post-DNB Heat-Transfer Model

The dependency of the heat-transfer coefficient on the velocity of the coolant, obvious from test results, is already understood in steady-state single-phase calculations, e.g., the well known Collburn equation. For the case of blowdown, a considerable quantity of droplets add to help cool the heated wall; therefore, an equation like the one mentioned would predict heat-transfer coefficients that are too low.

Therefore, for high void fraction, this equation was extended by Dougall and Rohsenow (1963), taking into account the liquid fraction of flow in the Re number.

$$\alpha = 0.023 \frac{\lambda_g}{D} \mathrm{Re}^{0.8} \mathrm{Pr}_g^{0.4} \qquad \mathrm{Re} = \frac{\dot{m} D}{\eta_g} \left[X + \frac{\rho_g}{\rho_l} (1 - X) \right] \tag{7}$$

Groeneveld (1972) proceeds in a quite similar manner, but adds a new factor:

$$\alpha = 0.00327 \frac{\lambda_g}{D} \mathrm{Re}^{0.901} \mathrm{Pr}_{g\,w}^{1.32} Y^{-1.5}$$
$$Y = 1 - 0.1 \left(\frac{\rho_l}{\rho_g} - 1 \right)^{0.4} (1 - X)^{0.4} \tag{8}$$

Both models had been tested under steady-state conditions. For the case of blowdown, in some tests big differences occur between measured and calculated heat-transfer coefficients, mainly in the first time with strong acceleration of flow. Therefore, a calculation model was developed considering in an additive manner the heat transport from wall to droplets that bound against this wall. This model is valid under the following conditions:

1 Rewetting of heated wall by droplets does not occur. This is usually attained at 2-4 s after onset of DNB.
2 Heat transfer to the droplets depends on liquid fraction present in the boundary layer at heated wall.
3 Heat transfer depends on size of droplets.

With these conditions, the heat transfer to the droplets can be calculated from

$$\alpha_{\mathrm{dr}} = C \frac{\lambda_{gw}}{d_{\mathrm{dr}}} (1 - \epsilon)^n \tag{9}$$

Droplet diameter is a function of We number

$$\mathrm{We} = \frac{d_{\mathrm{dr}} \rho_g w_{\mathrm{rel}}^2}{\sigma} \tag{10}$$

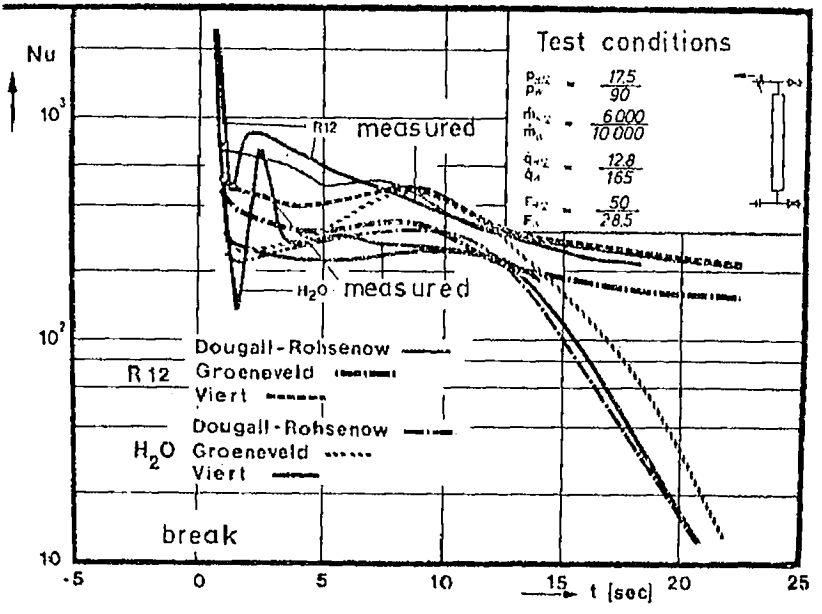

FIG. 20 Scaling tests in reactor emergency core cooling: comparison between measured and calculated Nu numbers.

whereas the relative velocity between both phases must be expre aid of slip:

$$w_{rel} = w_g - w_l = \left(1 - \frac{1}{S}\right)\frac{X\dot{m}}{\epsilon\rho_g}$$

For highly accelerated flow with a We number of 22 (Hinze, obtains the following equation:

$$\alpha = 0{,}023\ \frac{\lambda_g}{D}\left(\frac{X\dot{m}D}{\epsilon\eta_g}\right)^{0.8} Pr_g^{0.33}\left(\frac{\eta_g}{\eta_{gw}}\right)^{0.14} + 4.55\ \frac{\lambda_{gw}}{\rho_g\sigma}\left[\left(1 - \frac{1}{S}\right)\frac{X\dot{m}}{\epsilon}\right]^2 (1 -$$

A comparison of all three models is depicted in Fig. 20 for a \ corresponding Freon-test. Apart from the first seconds after on: when void fraction has relatively low values below $\epsilon < 0.8$ heat-transfer curves are reproduced for both fluids by all three mo accuracy of about 20 percent. This is valid for the time period past DNB.

REFERENCES

AEG-Bericht (1971). Hochdruckversuche des Notkühlprogramms für DW Programmbeschreibung.

AEG-E3-2560 (1972). Durchsatzmessung im Versuchskreislauf für Abblase Zweiphasenströmung.

Belda, W., and Viert, U.-P. (1974a). Theoretische und experimentelle Modellun zur Notkühlung, Zwischenbericht *RS* 48-03.

Belda, W., and Viert, U.-P. (1974b). Zwischenbericht *RS* 48-03.

Dougall, R. S., and Rohsenow, W. (1963). Film Boiling of the Inside of Vertic Upward Flow of the Fluid at Low Qualities. Report 9079-26, *MIT*.

Dukler, A. E. (1961). Comparison of Theoretical and Experimental Filr A.R.S.J., p. 86, Jan.

Groeneveld, D. C. (1972). The Thermal Behavior of a Heated Surface at Dryout, *AECL*-4309, Ontario.

Hinze, J. O. (1955). Fundamentals of the Hydrodynamic Mechanism of Splitting Processes, *AIChE J.*, vol. 1, p. 289.

KWU/R5-2885 (1974). Abschlussbericht über die Abblaseversuche mit 4-Stabl

Paleev, I. I., and Filipovich, B. S. (1965). Phenomena of Liquid Transfer i Dispersed Annular Flow, *Int. J. Heat Mass Transfer*, vol. 9, p. 1089.

Truong-Quang Minh. (1965). Some Hydrodynamical Aspects of Annul Flow Entrainment and Film Thickness, *Symp. on Two-Phase Flow*, Exeter